Influence of Sequence on the Self-Assembly of Peptide Nanoribbons on Silicon Substrates

A. Dhathathreyan* and B. U. Nair

Chemical Lab, CLRI (CSIR), Adyar, Chennai 600020, India

Received: September 20, 2010; Revised Manuscript Received: October 28, 2010

This work reports the formation of stable nanoassemblies of short pentapeptides LKLKL (pepI) and their mutated sequence LKKLL (pepII) obtained from their Langmuir−Blodgett films transferred onto hydrophilic and hydrophobic silicon substrates. The adsorption and assembly of the LB films of these peptides on solid surfaces have been studied by quartz crystal microbalance, surface plasmon resonance, and scanning electron microscopy. Both pepI and pepII assemble into nanosized ribbons, with diameters around 20−25 nm and lengths greater than 5 μm on hydrophobic surface, and tend to aggregate on hydrophilic surfaces with pepII showing twisted structures. Circular dichroic spectra of the films on a hydrophobic surface showed formation of a β-sheet-like structure, while the corresponding solution spectra did not show any specific secondary structure. Our results demonstrate the formation of a two-dimensional dense array of nanoassemblies with either vertical or horizontal patterns from such short peptides that may find application in nanotechnology.

Introduction

In the development of new nanomaterials, organizing objects at the nanoscale is of prime importance and is a key challenge in the applications area.[1−3] In this regard, biomolecules and their assemblies offer a very attractive template due to their inherent molecular recognition capabilities, biocompatibility, and the ease with which a bottom-up fabrication can be initiated.[4−9] A number of papers in the literature have reported the formation of specific designed nanoassemblies using short peptides and proteins and in the development of sensors.[10−14] By controlling the vapor−liquid−solid interface, highly oriented nanotubes or nanowires have been obtained using vapor deposition techniques. This technique works well with inorganic assemblies but is incompatible with biological or organic systems. In this regard, peptides as building blocks of nanomaterials are quite attractive in biotechnology applications. Rosenman et al. have reported strong piezoelectricity effects in peptide nanotubes.[15] A number of researchers have used simple dipeptide diphenylalanine as a template to grow nanotubes and have tested these tubes as templates for further growth of nanoclusters of metals, as containers to immobilize enzymes, as special materials showing high thermomechanical strengths, as motifs to grow new nanosized structures, as models for amyloid fibrils, and as models for collagen.[16−20] In most of these results, hollow tubular nanostructures are formed in aqueous solution by the self-association of the dipeptide, and the tubes are formed as individual entities and have a remarkable micrometer-scale persistence length.

In this work, we report the formation of ribbon-like structures of the peptide LKLKL and its mutated sequence LKKLL. These peptides are amphipathic and belong to the class of antimicrobial peptides (AMPs). AMPs have been shown to act as the first line of defense in almost all major groups of organisms like animals, plants, and microbes.[21,22] In recent years, AMPs have been implicated in several unexplained human inflammatory disorders. This has led to the search for novel therapeutic approaches.[23]

Because these peptides are amphipathic in nature, the organization of the peptides at the air/water interface as Langmuir films and as Langmuir−Blodgett (LB) films on solid silicon surfaces has been studied. Transfer of the LB films of these peptides and adsorption of the peptides on hydrophilic (oxide layer and alternating charged lipid multilayers) and hydrophobic solid surfaces without specific interactions were studied using circular dichroic spectroscopy (CD), quartz crystal microbalance (QCM), surface plasmon resonance (SPR), and scanning electron microscopy (SEM).

Experimental Section

PepI and pepII were bought from EZBiolab, U.S.A., and were 99.9% pure.

The neutral lipid dipalmitoylphosphatidylcholine (DPPC) and anionic lipid distearoylphosphatidic acid (DSPA) were from Larodan Chemicals, Sweden, and were 99.9% pure. Solvents for spreading the lipids (chloroform, toluene (99.7%), isopropanol (99.7%), and *n*-octadecyltrichlorosilane (98%)) were from Merck (Darmstadt, Germany). All chemicals were used without further purification. Deionized water from Millipore Milli-Q system was used for the preparation of the subphase buffers.

Surface Modification. The silicon wafers (Silchem Handelsgesellschaft GmbH, Freiberg,) used were first immersed in a mixture of H_2O, H_2O_2 (pa, 30% aqueous solution, Fluka), and NH_4OH (pa, 28% aqueous solution, Roth) (volume ratio of 5:1:1, heated to 80 °C for 10 min). Afterwards, the wafers were rinsed extensively and stored in water before coating. The polished surfaces of silicon substrates bear a native oxide layer. The oxide layer surface consists of siloxane bonds (Si−OSi) due to contact with the moisture from the atmosphere. After the above procedure, the silicon oxide surface is well-saturated with silanol groups, conferring very high hydrophilicity.

Silanization of silicon substrates was carried out with *n*-octadecyltrichlorosilane (OTS) dissolved in toluene at millimolar concentration.The substrates were first dried with nitrogen gas to eliminate the water and then immersed in the solution overnight at a temperature of 4 °C. The excess of OTS was removed by washing the substrates with toluene and isopropanol alternately several times.

* To whom correspondence should be addressed. Tel +91-44-24437167. Fax +91-44-24911589. E-mail aruna@clri.res.in, aruna.dhatha@gmail.com.

10.1021/jp1089678
Published on Web 11/16/2010

Langmuir and Langmuir−Blodgett films (LB films). The Langmuir films of the peptides have been spread from buffer solutions (millimolar) on the buffer subphase of pH = 7.4, lower than the isoelectric point of the two peptides (pI = 10.5), using a single barrier trough (model 601 S) from Nima Technology, U.K., connected to a thermostat. Concentrations of the peptides used were in the micromolar range. For the CD and SEM measurements, the LB films were then transferred to the freshly cleaned quartz substrate and the hydrophilic and hydrophobic silicon substrates at a surface pressure of π = 20 mN/m. The transfer ratio was around 0.85, and the transfer was usually Y-type.

Quartz Crystal Microbalance (QCM) Measurement. For QCM measurements, a 9 MHz AT-cut quartz crystal deposited with titanium and then gold as electrodes on both sides of the crystal was used as a substrate in a Maxtek instrument. The gold electrode surface was treated with piranha solution before use. The other side was covered with silicone rubber to avoid contact with any solution.

A mixed monolayer of DSPA and DPPC transferred onto a Au electrode plate of a 9 MHz QCM was used to examine the dynamics of the peptides binding onto the model membrane surface. A monolayer-transferred quartz crystal plate was soaked in 2 mL of 20 mM Tris-HCl buffer (pH 7.4). After stabilization of the frequency fluctuation, the solution of peptide was added to the buffer. Frequency and mass changes were monitored as the adsorption of the peptides took place. During measurement, the solution was not stirred to avoid the rapid aggregation of peptides.

Surface Plasmon Resonance (SPR) Measurement. SPR measurements were carried out using a BIAcore X instrument (BIAcore, Inc., Sweden) at 25 °C. The gold-coated substrate coated with three layers of the mixed system of DSPA + DPPC using a horizontal transfer technique of LB films was mounted onto a plastic cassette. The two peptide solutions (concentration, 2 μM) were made in 10 mM Tris-HCl buffer (pH 7.4) immediately prior to analysis. The buffer solution was filtered using Corning cellulose acetate membranes with 0.22 μm pores and degassed using a vacuum oven at 15−20 in. of Hg for 10 min, followed by sonication for 5 min. The measurement model was the multichannel model with a flow rate of 40 μL/min. At least two injections were done for each concentration. For all of the SPR measurement, glass substrates were coated with gold and then cleaned with 1:1:5 $NH_3OH/H_2O_2/H_2O$ for 10 minutes, flushed thoroughly with deionized water, and blown dry with nitrogen. For the hydrophobic surface, the chip was first silanized with OTS.

Data analysis was carried out with BIA evaluation 3.0 program.

Circular Dichroic Spectroscopy (CD) Spectra. The CD spectra of the LB films of pure peptides transferred to hydrophobic quartz substrates were obtained using a JASCO J-715 spectropolarimeter (JASCO Corp., Tokyo). The near-UV (340−250 nm) and far-UV (260−180 nm) spectra obtained were analyzed using the Selcon method,[24] fitting to three structural parameters, α-helix, β-sheet, and aperiodic. They were compared with the solution spectra.

Scanning Electron Microscopy (SEM). Scanning electron micrographs were obtained using a field emission scanning electron microscope (FE-SEM, Hitachi S-4200). The films transferred onto the substrates were dried in a desiccator for at least 1 h and then coated with gold prior to SEM observation.

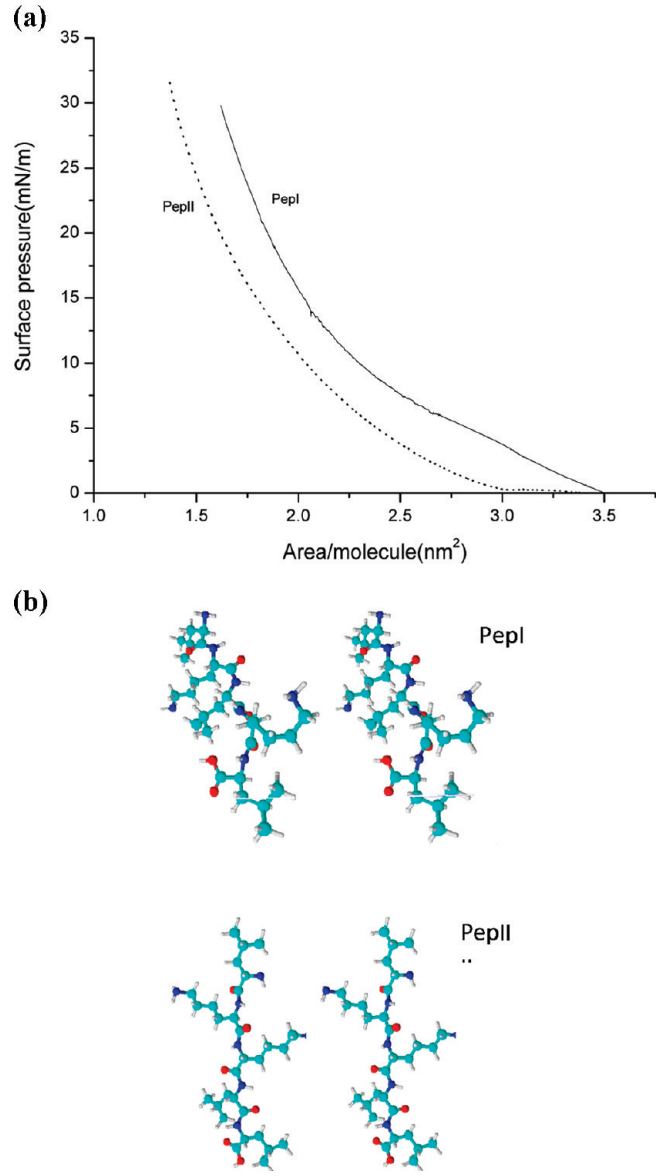

Figure 1. (a) Surface pressure−molecular area (π−A) isotherms of pepI and pepII spread on a subphase containing buffer (1 mM, pH = 7.4) at T = 22 °C. (b) Energy-minimized model for pepI and pepII at the interface.

Results and Discussion

Since both pepI and pepII are supposed to be amphipathic, the properties of their Langmuir films at the air/water interface were studied using surface pressure−molecular area isotherms of pepI and pepII measured at T = 22 °C. The isotherms in Figure 1a show a liquid-expanded (LE) to liquid-condensed (LC) state for both of the peptides. However, pepI shows a larger area compared to that of pepII, and this may arise due to the larger steric hindrance present in pepI compared with that in pepII. Figure 1b shows the energy-minimized assembly of pepI and pepII, and the average area measured at the air/water interface agrees quite well with the model.

To understand the rate of adsorption of the two peptides to solid surfaces, SPR measurements were performed, where the two peptide solutions were injected over the lipid-coated surface and a response was observed arising from the difference in the refractive indexes between the buffer and the peptide solutions. Figure 2 shows the typical SPR sensograms for the two peptides measured under continuous flow. PepI showed a faster rate of

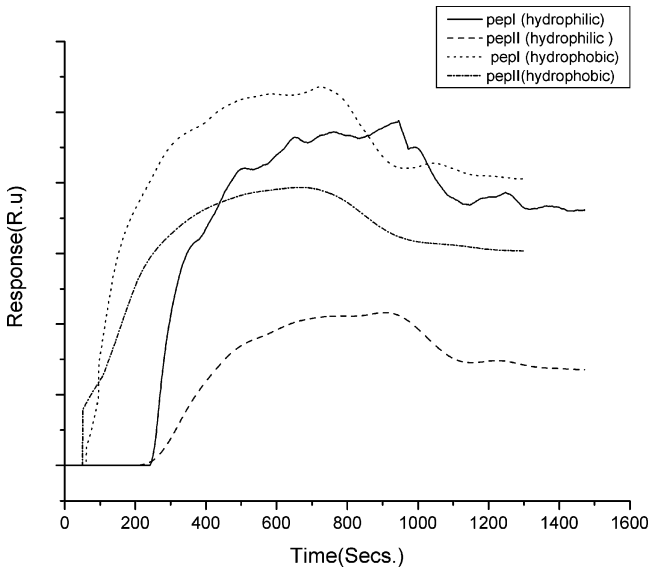

Figure 2. SPR sensograms for the two peptides measured under continuous flow on a DSPA+DPPC-coated surface; peptide concentration, 2 μM.

adsorption compared with that of pepII on both types of substrate. However, both peptides showed higher adsorption on the hydrophobic substrates.

Upon injection of a peptide-containing solution over the surface, there was a rapid signal response due to differences in the refractive indices of the buffer and peptide solution (1000 RU is a change in resonance angle of 0.1° and corresponds to a change in the index of refraction in solution of 0.0011) followed by a slower increase as the peptide adsorbed to the surface, eventually approaching steady state.

QCM was used to study the time course of frequency changes for pepI and pepII adsorbing to a DPPC+DSPA-coated quartz crystal, and the plots of the change in frequency and mass are presented in Figure 3a and b. These measurements were carried out without stirring of the solution because stirring causes convulsive aggregation of the peptides in bulk solution, leading to irregular adsorption. A calibration of the 9 MHz crystal showed that for a change of 1 Hz in frequency, the corresponding mass is around 6 ng/cm^2. In our study, we see that there is a change of about 22 Hz for pepI and around 18 Hz for pepII, reflecting a change of about 100−130 ng/cm^2 in mass. For a monolayer coverage of the two peptides, the mass change should be around 110 ng/cm^2, suggesting that these peptides form monolayers during adsorption. In this study, nonspecific binding of these peptides has not been considered specifically.

From both SPR and QCM studies, it is seen that the deposition rate of pepI is higher than that of pepII. This accelerated effect could have implication for amyloid formation.

CD was employed to assess the molecular configurations within the assembled nanostructures of two peptides transferred to the hydrophobic substrate. For this purpose, the quartz substrate coated with OTS was used, and the peptides were adsorbed to these surfaces. The CD spectrum shown in Figure 4 displays a positive peak at 195 nm and a negative peak at 220 nm, characteristic of the formation of the β-sheet structure. The solution spectra of the peptides did not show any specific feature. While such short peptides may not truly have typical secondary structural features in solution, in adsorbed films, local concentrations and organization may lead to such features.

In order to study the morphology of the peptides on solid surfaces, the films transferred onto the modified silicon substrates have been analyzed using SEM. Figure 5a and b shows the micrographs of pepI on hydrophilic and hydrophobic

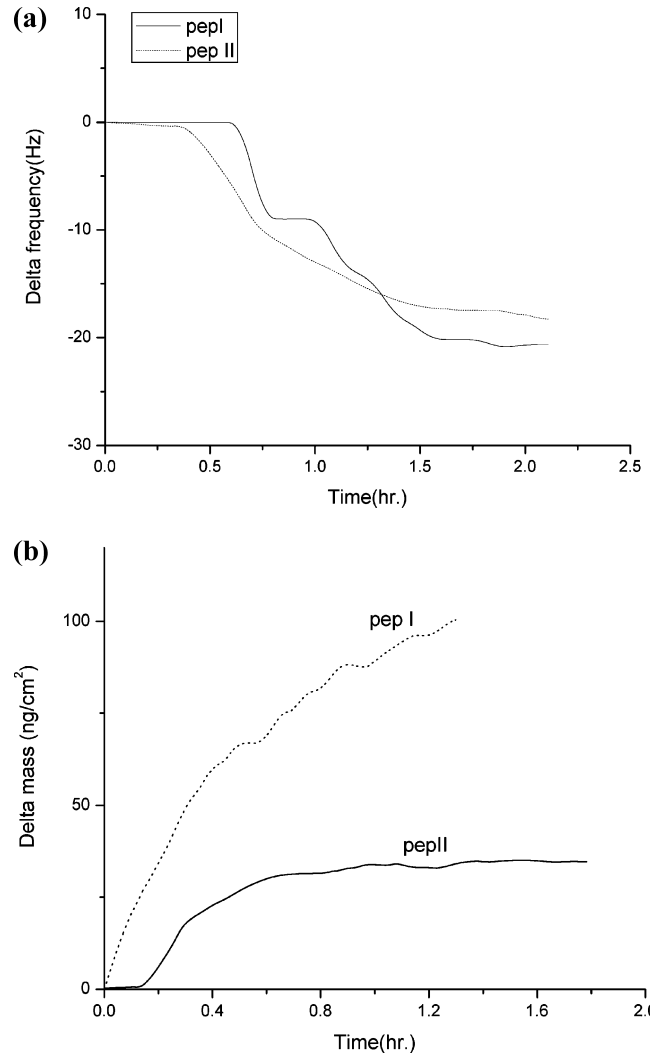

Figure 3. (a) Delta frequency versus time measurement. (b) Delta mass versus time measurement for pepI and pepII adsorbing to a DSPA+DPPC-coated quartz surface; T = 22 °C.

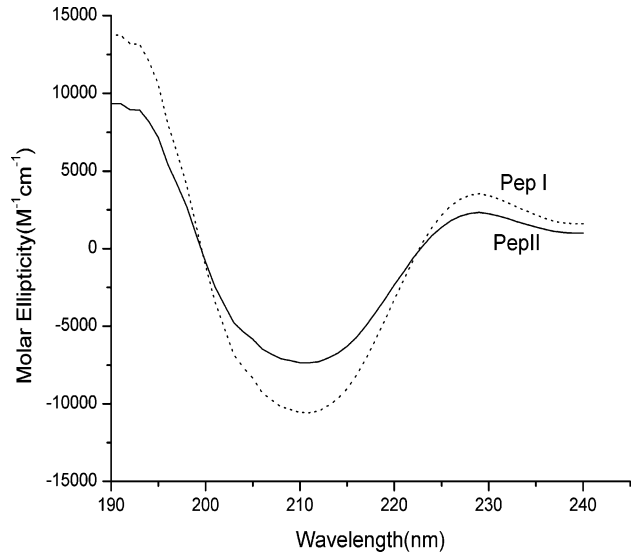

Figure 4. CD spectra of pepI and pepII adsorbed to a hydrophobic quartz surface.

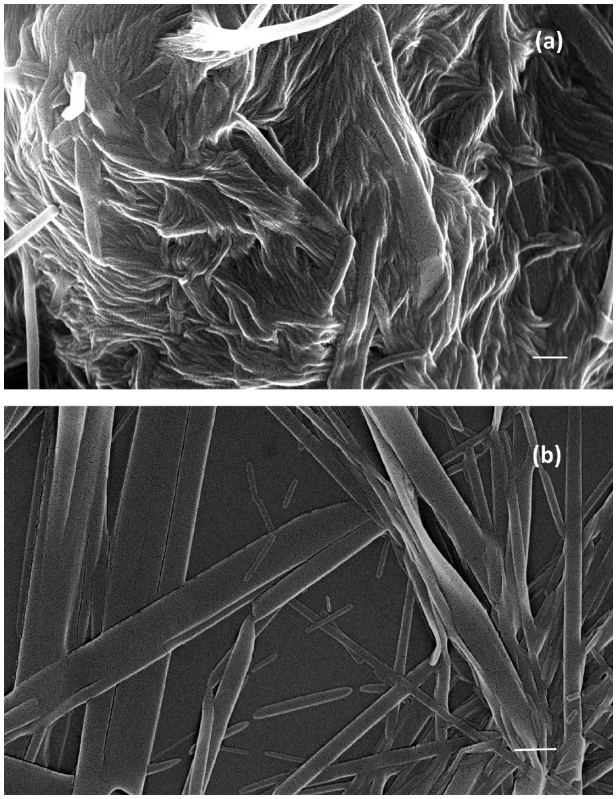

Figure 5. SEM of pepI films on (a) hydrophilic substrates (scale bar = 200 nm) and (b) hydrophobic substrates (scale bar = 1 μm).

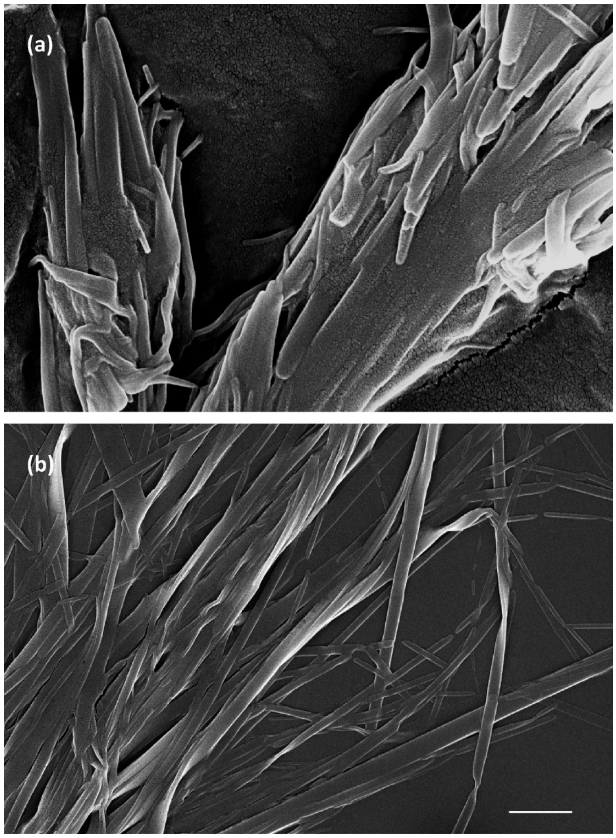

Figure 6. SEM of pepII films on (a) hydrophilic substrates (scale bar = 200 nm) and (b) hydrophobic substrates (scale bar = 1 μm).

substrates, and Figure 6a and b shows the micrographs corresponding to films of pepII on these substrates.

From the micrographs, it is seen that on a hydrophilic surface, both peptides exhibit aggregated structures, suggesting strong lateral adhesion. On a hydrophobic surface, the structures are less aggregated and appear ribbon-like. In the case of hydrophilic substrates, nonspecific adsorption can initially compete with the organization process and thus lead to uncontrolled growth of a possible amyloid-like structure. The nonfibril-like structure can initiate further aggregation on the membrane surface.

On the hydrophobic surface nanoribbon-like structures with no specific orientation are seen for both peptides, with approximate diameters of 20 nm. An impressive feature is that the lengths of these nanoassemblies mostly exceeded 5 μm.

This likely reflects the inability of the peptides to nucleate in an organized manner. Stabilization against clustering or bundling could well arise from the electrostatic repulsion associated with the presence of the alternating positively charged lysine groups in pepI, whereas in pepII, two adjacent lysines could prevent such packing.

In case of hydrophilic silicon surfaces, the surface carried a positive charge, and the peptides could not assemble into aligned arrays. Such surface-induced aggregation in biomolecules has been recently reported for fibrinogen[25] and in short peptide segments.[26]

In conclusion, the position and nature of the residue in the peptide determines the nature of the assembly. The controlled alignment of these highly ordered self-assembled peptide nanoribbons, which have unique chemical and mechanical stability, along with the ability to decorate them with functional groups may enable their integration into multiarray sensors, field-emission settings, and nanofluidic devices.

Acknowledgment. The authors would like to thank the Nano mission of DST, Govt. of India, for a project grant under which part of the work was carried out.

References and Notes

(1) Zhong, Z. H.; Wang, D. L.; Cui, Y.; Bockrath, M. W.; Lieber, C. M. *Science* **2003**, *302*, 1377.
(2) Modi, A.; Koratkar, N.; Lass, E.; Wei, B. Q.; Ajayan, P. M. *Nature* **2003**, *424*, 171.
(3) Patolsky, F.; Zheng, G.; Hayden, O.; Lakadamyali, M.; Zhuang, X.; Lieber, C. M. *Proc. Natl Acad. Sci. U.S.A.* **2004**, *101*, 14017.
(4) Whitesides, G. M.; Mathias, J. P.; Seto, C. T. *Science* **1991**, *254*, 1312.
(5) Sarikaya, M.; Tamerler, C.; Jen, A. K.; Schulten, K.; Baneyx, F. *Nat. Mater.* **2003**, *2*, 577.
(6) Ghadiri, M. R.; Granja, J. R.; Milligan, R. A.; McRee, D. E.; Hazanovich, N. *Nature* **1993**, *366*, 324.
(7) Cui, H.; Muraoka, T.; Cheetham, A. G.; Stupp, S. I. *Nano Lett.* **2009**, *9*, 945.
(8) Matsui, H.; Gologan, B. *J. Phys. Chem. B* **2000**, *104*, 3383.
(9) Matsui, H.; Douberly, G. E. *Langmuir* **2001**, *17*, 7918.
(10) Ulijn, R. V.; Smith, A. M. *Chem. Soc. Rev.* **2008**, *37*, 664.
(11) Xu, H.; Wang, J.; Han, S.; Wang, J.; Yu, D.; Zhang, H.; Xia, D.; Zhao, X.; Waigh, T. A.; Lu, J. R. *Langmuir* **2009**, *25*, 4115.
(12) Lu, J. R.; Perumal, S.; Hopkinson, I.; Webster, J. R. P.; Penfold, J.; Hwang, W.; Zhang, S. *J. Am. Chem. Soc.* **2004**, *126*, 8940.
(13) Deng, M.; Yu, D.; Hou, Y.; Wang, Y. *J. Phys. Chem. B* **2009**, *113*, 8539.
(14) Castelletto, V.; Hamley, I. W.; Cenker, C.; Olsson, U. *J. Phys. Chem. B* **2010**, *114*, 8002.
(15) Kholkin, A.; Amdursky, N.; Bdikin, I.; Gazit, E.; Rosenman, G. *ACS Nano* **2010**, *4*, 610.
(16) Czajlik, A.; Beke, T.; Bottoni, A.; Perczel, A. *J. Phys. Chem. B* **2008**, *112*, 7956.
(17) Sedman, V. L.; Allen, S.; Chen, X.; Roberts, C. J.; Tendler, S. J. B. *Langmuir* **2009**, *25*, 7256.
(18) Yu, L.; Banerjee, I. A.; Gao, X.; Nuraje, N.; Matsui, H. *Bioconjugate Chem.* **2005**, *16*, 1484.
(19) George, J.; Thomas, K. G. *J. Am. Chem. Soc.* **2010**, *132*, 2502.

(20) Abramovich, L. A.; Reches, M.; Sedman, V. L.; Allen, S.; Tendler, S. J. B.; Gazit, E. *Langmuir* **2006**, *22*, 1313.
(21) Gallo, R. L.; Murakami, M.; Ohtake, T.; Zaiou, M. *J. Allergy Clin. Immunol.* **2002**, *110*, 823.
(22) Hancock, R. E.; Diamond, G. *Trends Microbiol* **2000**, *8*, 402.
(23) Brogden, K. A. *Nat. Rev. Microbiol.* **2005**, *3*, 238.
(24) Sreerama, N.; Woody, R. W. *Anal. Biochem.* **1993**, *209*, 32.
(25) Sankaranarayanan, K.; Dhathathreyan, A.; Miller, R. *J. Phys. Chem. B* **2010**, *114*, 8067.
(26) Xu, H.; Wang, Y.; Ge, X.; Han, S.; Wang, S.; Zhou, P.; Shan, H.; Zhao, X.; Lu, J. R. *Chem. Mater.* **2010**, *22*, 5165.

JP1089678